Progress in Superconductivity Vol.13 No.3 pp.151-157 30 April 2012

2-Dimensional Numerical Studies on Thin HTS Film under Time Varying Magnetic Field Using Finite Element Method

K. S. Kwak[*,a], H. Y. Lee[a], J. K. Rhee[a], D. Youm[a], J. Yoo[*,+,b], Y. H. Han[c], B. J. Park[c]

[a] *KAIST, Daejeon, Korea*

[b] *Chonbuk National University, Jeonju, Korea*

[c] *Green Growth Lab. KEPRI, 305-380 Daejeon, Republic of Korea*

(Received 21 February 2012; revised 16 April 2012; accepted 17 April 2012)

변화하는 자기장 하에 있는 고온초전도체에 대한 유한요소법을 이용한 2차원 수치해석 연구

곽기성[*,a], 이효연[a], 이준규[a], 염도준[a], 유재은[*,+,b],한영희[c], 박병준[c]

Abstract

In this paper, we used E-J constitutive law and H-formulation to calculate magnetic field profile, current density, and magnetization of high temperature superconductor (HTS) placed in time varying applied magnetic field. Finite element method (FEM)-based software, *Comsol Multiphysics 3.5a*, was employed to simulate 2-dimensional model of a superconducting thin strip. The numerical results based on Kim's critical state model were compared with the case of strip in a perpendicular field in the Brandt's paper as well as experimental data observed by Scanning Hall Probe and SQUID.

Keywords : HTS film, Finite Elements Method, 2-dimensional modeling

I. Introduction

In practical applications, type II superconductors have many advantages, such as high transition temperature, ability to carry large currents, ability to operate in an external field and stable levitation phenomenon originating from interaction with permanent magnets. In order to implement and optimize the devices containing high temperature superconductors (HTS), it is indispensable to understand their electro-magnetic properties. Superconductors expel external magnetic field, *i.e.* the field cannot penetrate into them. This phenomenon is called Meissner effect. The expelled flux is accumulated at the edges of the superconductors because supercurrent flows around them. These supercurrent and expelled flux vary depending on each

*Corresponding author. Fax : +82 42 350 5330

e-mail : jaeunyoo@hotmail.com

+On leave from KAIST High temperature superconductor and nano-complex material lab

other and the applied field intensity and history. This hysteretic behavior of the magnetic flux is complicated and is a basis of ac loss.

To describe the field and current distributions of the HTS in a critical state, several critical state models have been proposed with particular relationships between the field and critical current density. The most popular one is the concept of critical state introduced by Bean [1], which assumes that the critical current density is constant and independent of the external field. Another original critical state model is Kim's model including field dependence of the critical current density [2]. In practical point of view, however, those critical state models are too simple to analyze the HTS system known to have a highly nonlinear property described by E-J power law with a finite n-value [3]. The most effective way to handle this nonlinearity is to use some iteration, for example, finite element method (FEM) with A-V formulation (which is based on A-magnetic vector potential and V-electric potential difference) [4, 5], unconstrained H-formulation (which is based on H-magnetic field) [6], or T-Φ formulation (which is based on T-current vector potential and Φ-electric potential) [7, 8]. To describe the electromagnetic properties of superconductors, those formulations include Maxwell's equations combined with the critical state model.

In the present paper, the H-formulation and the E-J power law combined with Kim's critical state model were calculated to obtain the field and current density distributions and the MH-curves of the HTS thin strip under time varying magnetic fields using general time dependent partial differential equation mode (PDE mode) in FEM-based software, Comsol Multiphysics 3.5a.

The model has been constructed in correspondence with $SmBa_2Cu_3O_7$ coated conductor grown on an ion beam assisted deposition (IBAD) template by co-evaporation method so that the results extracted from the simulations can be directly compared with the experimental data on $SmBa_2Cu_3O_7$ coated conductor measured with scanning hall probe [9] and SQUID. The results show that the demagnetization factors are automatically taken into account when the governing equations were solved with a given geometry. The resultant current density and field profiles were not exactly the same as experimental data, because the inhomogeneity considered as an important feature of a coated conductor [10] was ignored in our calculations.

II. Superconducting Modeling

Since the coated conductor is long and straight, it can be assumed as an infinitely thin slab so that we can use 2-dimensional analysis with two dependent variables, H_x and H_y. As shown in Fig. 1, the model is composed of two domains; domain 1 is a circular normal region with radius 2 cm and domain 2 is a thin strip shaped superconducting region with dimension 4 mm × 22 μm (Although the thickness of the real sample is 2.2 μm, we used 22 μm, which is the thickness limit in the calculation without any convergence problem with appropriate time steps of 10^{-6} sec order. Because of the thin film geometry, the high aspect ratio produces a large number of nodes that introduce calculation time and convergence issue [11]). Each domain has its own electrical property expressed by the E-J relationship. The normal region, which we assumed is air, follows Ohm's law $E = \rho_{air} \cdot J$ and the HTS region has nonlinear property expressed by

$$\boldsymbol{E} = E_c \left(\frac{J}{J_c} \right)^n = \left[\frac{E_c}{J_c} \left(\frac{J}{J_c} \right)^{n-1} \right] \boldsymbol{J} = \rho J \qquad (1)$$

n = 21 was adopted as the exponent value according to the fitting result of the I-V-curve of typical type II superconductors. E_c = 10 μV/cm is the critical electric field and J_c is the critical current density. The external field was set in the direction of the y-axis in Figure 1, that is, normal to the superconductor surface in the form of sinusoidal wave in time.

$$H_{app}(t) = H_0 \sin(2\pi f t) \qquad (2)$$

where the frequency is 50 Hz.

In fact, this method does not consider the creep effect, so the frequency related to the flux creep has no impact on the results [12]. The magnetization of superconductors depends on the previous history of the applied field. Therefore we calculated the field distribution of the superconductor for at least two periods of the time variation of the external field.

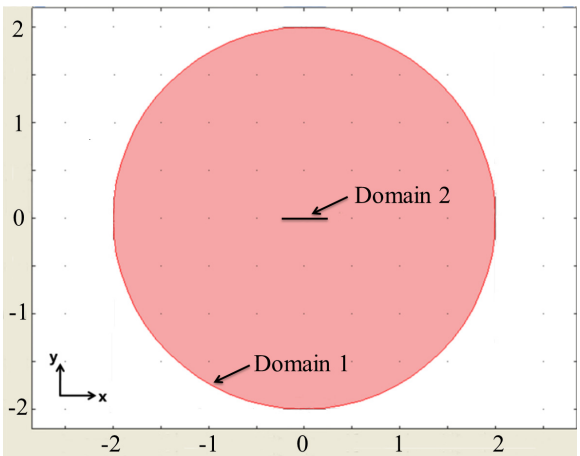

Fig. 1. The 2-dimensional model geometry consisting of two subdomains : subdomain 1 is the circular normal region (radius = 2 cm) and subdomain 2 represent the HTS thin strip cross section of 4 mm - width and 22 μm - thickness assumed as the infinite length.

2.1 Equations and Boundary Conditions

For the analysis of electromagnetic behaviors of the HTS thin strip, solutions of Maxwell's equations are required. With quasi-static approximation, Faraday law and Maxwell-Ampere law can be written as

$$\nabla \times \mathrm{E} = -\frac{\partial \mathrm{B}}{\partial t} \tag{3}$$

$$\nabla \times \mathrm{H} = \mathrm{J} \tag{4}$$

and according to the H-B constitutive law,

$$\mathrm{B} = \mu_0 \mathrm{H} \tag{5}$$

Partial differential equations for each domain derived from these basic equations can be solved with suitable boundary conditions. Dirichlet boundary conditions were used to both boundaries: the boundary condition between the two domains is the continuity of the tangential component of the magnetic field.

$$0 = \mathrm{n} \times (\mathrm{H}_1 - \mathrm{H}_2) \tag{6}$$

where n is the unit vector normal to the boundary.

The outer boundary condition is set as

$$0 = \mathrm{H} - \mathrm{H}_{\mathrm{app}} \tag{7}$$

To apply a perpendicular magnetic field in the form of Eq. (2) with $\mu_0 H_0$ = 3600 Gauss, outer boundary conditions were established as

$$0 = H_x, \quad 0 = H_y - H_{app} \tag{8}$$

2.2 Mesh Properties and Time step

With finite element software, one can generate a free mesh very easily. The unit mesh shape chosen was triangle as shown in Fig. 2. The resolution of the mesh in the narrow region (subdomain 2) was 2 in the simulation. As mentioned in Section 2, the high aspect-ratio of the thin strip geometry increases the number of nodes, resulting in extremely long computational time and diverging solver. Hence optimizing the ratio of width to thickness of the thin strip is necessary. Though, for a better comparison, we have chosen a relatively high ratio at the cost of solving time.

As can be seen from Fig. 2, the mesh quality near the HTS thin strip can be enhanced selectively, helping solver to operate more efficiently. The time step setting also influences the convergence rate and stability of the iterative system. In our model, the range of maximum time step ensuring that the solver system converges to the reliable solutions was 2 μs to 10 μs.

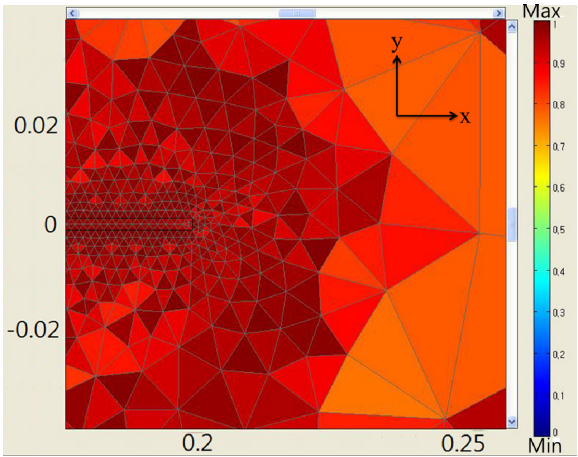

Fig. 2. Mesh with triangular elements. On the right side, the scale bar expresses the mesh quality, which is good in general, especially near the subdomain 2, HTS thin strip region. The x and y represent the coordinate values of the model geometry.

2.3 Sample properties and Kim's model

As depicted in Fig. 3, the critical current (I_c) versus applied magnetic field (B_{app}) obtained from the previous experiment in [9] provides the fact that J_c has a strong field dependent property. Hence we can assume that J_c is well explained by Kim's critical state model

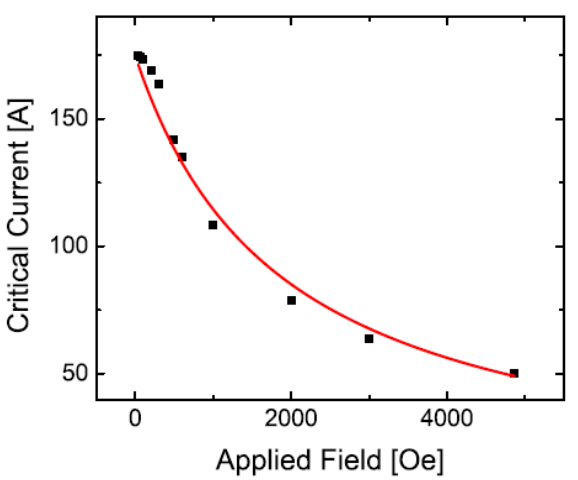

Fig. 3. Critical current (I_c) versus applied magnetic field (B_{app}) measured on the $SmB_2Cu_3O_7$ coated conductor under out-of-plane magnetic field.

$$J_c(B) = \frac{J_{c0}}{1 + B / B_k} \tag{9}$$

Fitting the I_c-B_{app} curve to Eq. (9), the values of parameters, $J_{c0} = 2 \times 10^6$ A/cm^2 and $B_k = 1800$ Gauss were obtained.

III. Results and Discussion

Initially, the magnetization curves obtained from the calculation and the SQUID measurement were compared in order to confirm the validity of the model, and these are shown in Figures 4 (a) and (b), respectively. The magnetic moment, **m**, of the HTS was integrated using the calculated current density distributions, which is described as

$$\mathrm{m} = \int_{Domain2} \frac{1}{2} \mathrm{r} \times \mathrm{J} d^2 r \tag{10}$$

The integration formula over subdomain is easily implemented in the software.

As mentioned in Section 2, due to the convergence issue and to minimize the calculation time, the thin strip dimensions were determined as 4 mm (width) × 22 μm (thickness) with infinite length. For the calculation, the input value of the critical current density was the same as the sample's J_c. The current that can flow in the model is ten times higher than the experimental values. Hence it is difficult to compare the absolute values of the data obtained from the calculation and the SQUID measurement. Instead, the simulated magnetization loop in Fig. 4a has a qualitatively similar shape to the measured curve in Fig. 4b, from which we can assure the validity of this approach.

Next, we compared the field distributions measured using a scanning Hall probe system with those calculated. For that, the characteristic field parameter defined as $H_c = K_c/\pi$, was introduced, where K_c is sheet current density, ($K_c = j_c \cdot d$, where j_c is critical current density and d is thickness of sample). The K_c and H_c values of SmBCO sample are

140.3 A/cm and 176.4 gauss, respectively. During the experiment, the external field was increased from 0 to 450 gauss in 90-gauss steps. The maximum external field and increment values correspond to about 2.5 H_c, and 0.5 H_c, respectively. For the simulation, H_a was increased in the same way where the H_c of the model was 1764 gauss.

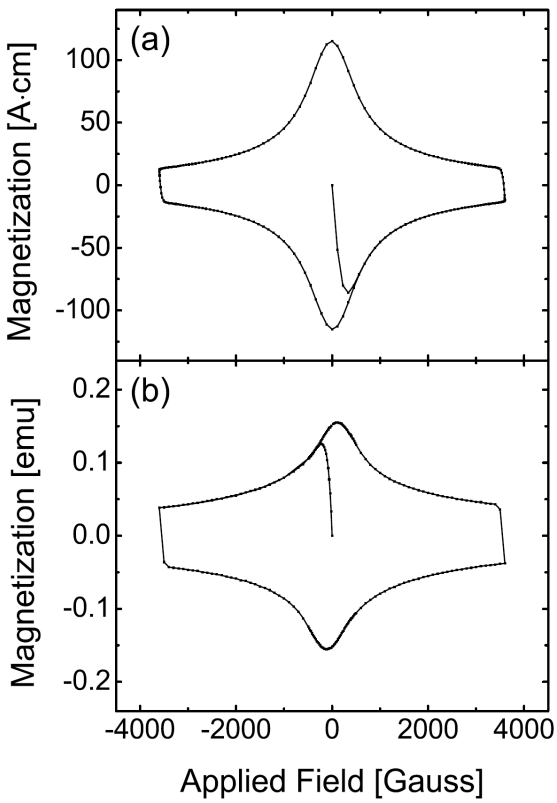

Fig. 4. (a) The magnetization loop from the Kim's model combined simulation of the HTS thin strip under the out-of-plane field. (b) Measured magnetization loop of the $SmBa_2Cu_3O_7$ coated conductor.

Figure 5 (a) and (b) show the results of field distributions obtained from the calculation and SHP measurement, respectively.

The field distribution in Figure 5(c) was predicted theoretically by Brandt and Indenbom [13]. As shown in Figure 5, the simulated results agreed with those from the measurement and theoretical calculations overall. In Fig. 5a, the resulting field profiles, H(x), of the simulation at y = 0 are shown. Fig. 5a shows that, under the applied field, the magnetic flux penetrates from the edges to the critical state region and decay inside the sample, forming a Meissner state region with no flux. By increasing the applied field, the penetration depth extends further inside the sample as can be seen from Fig 5a.

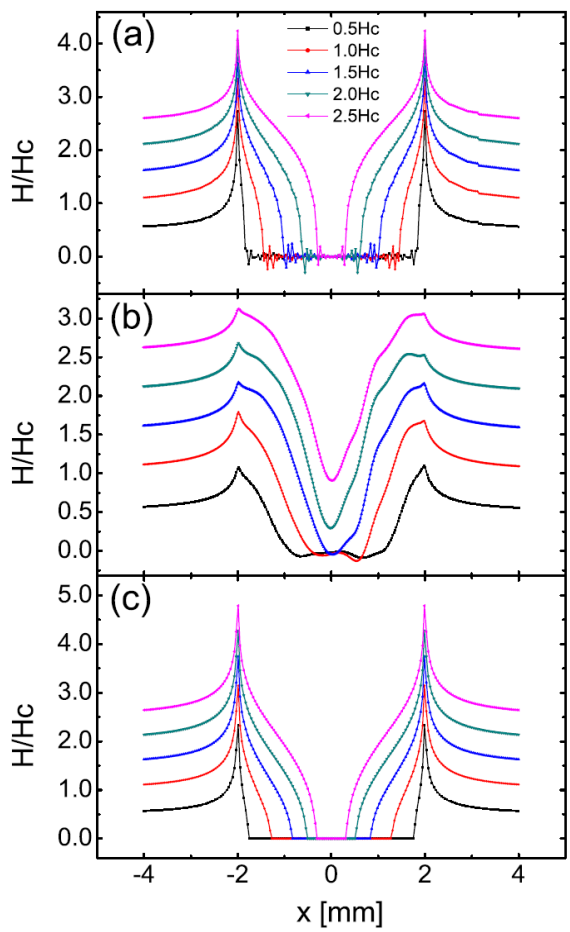

Fig. 5. The distributions of the magnetic field component perpendicular to the surface of the HTS tape when subjected to the out-of-plane field increased from $0.5H_c$ to $2.5H_c$ (where H_c of the $SmB_2Cu_3O_7$ coated conductor is $H_c = J_{c0}\cdot d/\pi$) obtained from (a) the FEM-based simulation, (b) the measurements using the scanning hall probe method [9] and (c) the Brandt and Indenbom's analytical solutions [13]. (From the bottom to the top of the data, the external field applied is 0.5, 1.0, 1.5, 2.0, 2.5 H_c)

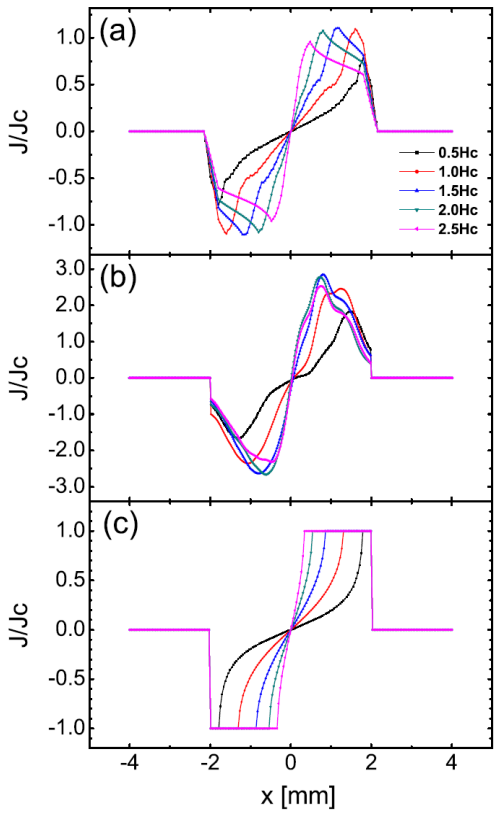

Fig. 6. The distributions of z-component sheet current density in the same condition with Fig. 5 resulting from (a) the simulation, (b) the experiment, and (c) Brandt's paper.

These features appeared in the measurements performed in [9] as well as Brandt and Indenbom's analytical solutions [13] illustrated in Fig. 5b and c, respectively. The differences in the detailed curvature of the field profiles can become explicit by calculating the current density distributions. Since the thin strip in our model has a non-trivial thickness, current density distributions in various y-positions in the superconducting region were extracted and integrated to calculate the sheet current densities shown in Fig. 6a. Comparing the current distributions, it becomes evident that the field dependence of J_c is necessary for analysis of the current profiles. In Brandt and Indenbom's solution assuming constant J_c in Fig. 6c, the sheet current density profiles remain constant in the entire critical state region. In the case of the simulation based on Kim's model, on the contrary, the decrease of J(x) near the edges appears clearly. It is due to the J_c decrease in magnetic field, hence in the experimental results in Figure 6(b), the decrease of the J_c values at the edges might arise not only from the poor quality of the edges [14], but also from the field dependence of J_c. Secondly, the measured current densities have the most intense values at the boundaries between the Meissner and the critical state, as can be seen in detail in Fig. 7. The J_c (x) maximum, for example, in the case of the $H_a = 2.5\ H_c$ is exhibited at x = ± 1 mm, which is the boundaries of two regions. That is because the current density was caused by the field gradient as well as the curvature, that is, $J = \nabla \times \mathbf{B} = (\nabla B) \times \hat{n} + B(\nabla \times \hat{n})$. Clearly, ∇B and $\nabla \times \hat{n}$ have the maximum values at the boundaries of the Meissner and the critical region.

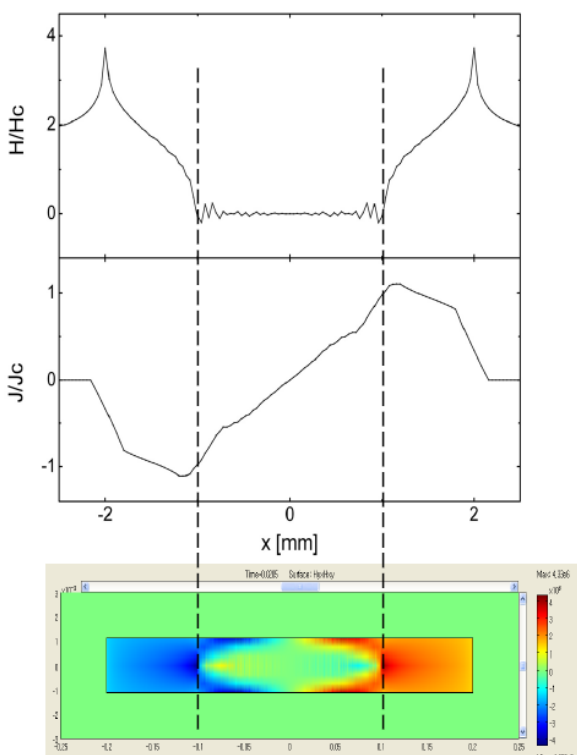

Fig. 7. Numerical results of the field and the sheet current distributions and, at the bottom, the 2-dimensional plot of the current density when $H_0 = 1.5H_c$ is applied in y direction.

However, there are several features in the measurement that we could not understand solely from the field dependence of J_c. For example, in contrast to the simulated J(x), the measured J(x) has many detailed curves and has its maximum values becoming higher with increasing external field. We conjecture that this feature of measured J(x) might be caused by the granular structure of the coated conductor because we have disregarded the granular structure of the coated conductor in our modeling. Nevertheless, in general, the HTS properties were calculated successfully in the simulation.

IV. Conclusions

In conclusion, we have completed 2-dimensional numerical studies on an HTS thin strip under time varying out-of-plane magnetic field using FEM-based software, Comsol Multiphysics 3.5a. Combining the E-J power law and Kim's critical state model, the calculated magnetization curve was in good agreement with the measured data, which confirms the accuracy of the present method. We have found that, based on the concept of the field dependent property of the critical current density, the decreases near the edges of the current densities measured by the scanning hall probe can be explained.

Acknowledgements

This work was supported by Basic Science research Program through the National Research Foundation (NRF) funded by the Ministry of Education, Science and Technology (MEST) (NRF-2011-R1A4A003-2011-0013170).

This work was supported by a Grant from Electric Power Industry Technology Evaluation and Planning Center (ETEP), Republic of Korea.

References

[1] Bean C. P, Phys. Rev. Lett. 8 (1962) 250.
[2] Kim Y. B, Hampstead C F and Strnad A R, Phys. Rev. Lett. 9 (1962) 306-309.
[3] Rhyner J, Physica C 212 (1993) 292.
[4] Ruiz-Alonso D, Coombs T, Cambell A M, Supercond. Sci. Technol. 17 (2004) 305-310.
[5] Barnes G, McCulloch M, Dew-Hughes D, Supercon. Sci. Technol. 12 (1999) 518-522.
[6] Pecher R, McCulloch M D, Chapman S J, Prigozhin L, Elliottk C M, 6th European Conf. on Applied Superconductivity (EUCAS2003).
[7] Meunier G, Le Floch Y, Guérin C, IEEE Trans. Magn, 39 (2003) 1729-1732.
[8] Amemiya N, Miyamoto K, Banno N, Tsukamoto O, IEEE Trans. Appl. Supercond. 7 (1997) 2110-2113.
[9] Jaeun Yoo, Jaeyoung Lee, Dojun Youm, Journal the Korean Physics Society. Vol. 51, No. 5 (2007) 1776-1781.
[10] Johansen T H, Baziljevich M, Bratsberg H, Galperin Y, Lindelof P E, Shen Y, Vase P, Phys. Rev. B 54 (1993) 16264.
[11] Francesco Grilli, Andrea Lcarelli, Gunter Lüpke, Timothy Haugan, Paul Barnes, Comsol Conference 2008 Boston.
[12] Z Hong, A M Campbell, T A Coombs, Supercond. Sci. Technol. 19 (2006) 1246-1252.
[13] E. H. Brandt, M. Indenbom, Phys. Rev. B 48 (1993) 12893.
[14] Amemiya N, Shinkai Y, Iijima Y, Kakimoto Y, Takeda K, Supercond. Sci. Technol. 14 (2001) 611-617.